

Decoration of single-walled carbon nanotubes with Pt nanoparticles from an organometallic precursor

E. Ramírez-Meneses · V. Montiel-Palma ·
V. H. Chávez-Herrera · J. Reyes-Gasga

Received: 30 October 2010 / Accepted: 12 January 2011 / Published online: 29 January 2011
© Springer Science+Business Media, LLC 2011

Abstract Carbon nanotubes (CNTs) are nanomaterials of high interest due to their unique structural, electrical, and mechanical properties. Carbon materials have been widely employed to support metallic nanoparticles for catalysis and electrochemical applications. In this work, we investigated the synthesis of platinum nanoparticles generated from the complex $\text{Pt}_2(\text{dba})_3$ (tris(dibenzylideneacetone) diplatinum) and stabilized with a long alkyl chain amine, hexadecylamine (HDA) and supported on functionalized single-walled carbon nanotubes (SWCNTs). High resolution transmission electron microscopy (HRTEM) studies revealed isolated Pt nanoparticles (2–3 nm) on SWCNTs. Powder X-ray diffraction (XRD) was used to assess the structure of Pt nanoparticles dispersed on SWCNTs assigned to Pt face-centered cubic (fcc). Additionally, infrared Fourier transform spectroscopy confirmed the presence of the stabilizer at the surface of the Pt nanoparticles even after the purification step and functional

groups at the surface of pre-treated SWCNTs. This synthetic method may be an alternative route to prepare small size Pt nanoparticles supported on functionalized SWCNTs.

Introduction

Since their discovery, carbon nanotubes (CNTs) have received much attention due to their exceptional mechanical, electronical, and thermal properties [1, 2]. CNTs can be used in a wide range of fields, including chemical, electrical, and mechanical applications and offer great promise as basic materials at the core of materials nanotechnology. In particular, CNTs find applications in batteries, flat panel displays, chemical sensors, nanoelectrical devices, mechanical reinforcement, supports of catalysts or electrocatalysts, etc. [3–5]. For this reason, there are an increasing number of synthetic procedures to functionalize or decorate CNTs with metal or metal oxides nanoparticles. Among these, chemical reduction [6, 7], chemistry precipitation [8, 9], supercritical carbon dioxide deposition [10], electrodeposition [11], and hydrothermal synthesis [12] have been developed. CNTs as nanostructured supports for Pt utilization have received increasing attention since the 1990s due principally to their unique surface structure, high electric conductivity, and large surface areas. One of the main purposes of using CNTs-supported Pt nanoparticles are the reduction of Pt loading and improve performance for several applications [13, 14]. An interesting review about the progress in the synthesis of CNT-supported Pt nanoparticles has been published by Lee et al. [15]. This review covers the different chemical and electrochemical strategies used to obtain these materials, as electrocatalysts. Among these, the electro-deposition

E. Ramírez-Meneses
Departamento de Ingeniería y Ciencias Químicas, Universidad Iberoamericana, Ciudad de México, Prolongación Paseo de la Reforma 880, C.P. 01219 Lomas de Santa Fe, Mexico

E. Ramírez-Meneses (✉) · V. H. Chávez-Herrera
Centro de Investigación en Ciencia Aplicada y Tecnología Avanzada, CICATA-IPN Unidad Altamira, Carretera Tampico-Puerto Industrial, C.P. 89600 Altamira, Tamaulipas, Mexico
e-mail: esther.ramirez@uia.mx

V. Montiel-Palma
Centro de Investigaciones Químicas, Universidad Autónoma del Estado de Morelos, Av. Universidad 1001, Colonia Chamilpa, C.P. 62201 Cuernavaca, Morelos, Mexico

J. Reyes-Gasga
Instituto de Física, Universidad Nacional Autónoma de México, C.P. 04510 Ciudad Universitaria, D.F., Mexico

method is the most widely used for highly dispersed Pt nanoparticles on CNTs. On the other hand, sonochemical, microwave heated polyol process, electro-deposition, sputter-deposition, and γ -irradiation techniques can also produce dispersed Pt nanoparticles with small sizes. The most widely employed precursors for this preparation of nanosized Pt particles by the above mentioned methods have been principally H_2PtCl_6 , K_2PtCl_4 , and $PtCl_2$ [6, 16–20]. Other less common precursors have also shown high dispersion of Pt nanoparticles. Bayrakceken et al. [10] reported the use of $PtMe_2COD$, ($COD = 1,5$ -cyclooctadiene) as precursor to decorate multi-wall carbon nanotubes with platinum nanoparticles having an average size of 2 nm by supercritical carbon dioxide deposition. Zhang et al. reported the synthesis of close packed polyacrylonitrile nanofibers containing platinum (II) acetylacetone by polymerization of acrylonitrile in a porous anodic aluminum oxide template. Subsequent pyrolysis resulted in carbon nanofibers wherein the Pt(II) compound, $Pt(acac)_2$ was reduced *in situ* to form Pt nanoparticles dispersed throughout the carbon nanofibers and having a size range of 1–4 nm [15, 21]; other synthesis using the same precursor has been also reported [22]. More recently, Guzman et al. described the synthesis of Pt nanoparticles from dihydrogen dinitrosulfonateplatinum, $H_2Pt(NO_2)_2SO_4$ as precursor and $NaBH_4$ as reducing agent. The obtained Pt nanoparticles showed an average size between 60 and 90 nm and were employed to construct composites with dopamine using the cyclic voltammetry technique. The composites were employed to modify glassy carbon electrodes with and without multiwall carbon nanotubes [23]. On the other hand, an interesting work was reported by Solla-Gullón et al. The authors obtained Pt nanoparticles supported on single-walled carbon nanotubes (SWCNTs) by solid-state reaction between the SWCNTs and two different Pt precursors, bis(dibenzylideneacetone) platinum, $Pt(dba)_2$ or tri(dibenzylideneacetone) platinum, $Pt(dba)_3$. Pt nanoparticles showed a particle size of 2.5 nm [24]. At this point, alternative precursors and different routes to obtain Pt nanoparticles highly dispersed on CNTs are still widely studied. Taking into account the previous synthesis of Pt nanoparticles from the $Pt_2(dba)_3$ precursor using amines as stabilizers by the organometallic approach described by Chaudret and one of us [25, 26], the authors describe in the present work the synthesis of platinum nanoparticles from the same organometallic precursor decomposed under H_2 in the presence of hexadecylamine (stabilizer) and SWCNTs. This synthesis generated well dispersed isolated Pt nanoparticles (2–3 nm) as confirmed by high resolution transmission electron microscopy (HRTEM). Additionally, structural analysis by X-ray diffraction (XRD) and FT-IR measurements on the stabilized Pt nanoparticles dispersed on SWCNTs were also carried

out after the purification steps. This synthetic method may be highly promising as an alternative route to prepare small size Pt nanoparticles supported on functionalized SWCNTs.

Experimental

Pretreatment of SWCNTs

The surface of commercial SWCNTs makes difficult substrate on which to attach metal nanoparticles; physisorbed Pt nanoparticles can be easily removed under agitation. Previous reports have suggested, chemically anchor Pt or stabilized Pt nanoparticles onto the surface of the SWCNTs using a process of wet oxidation involved refluxing SWCNTs in nitric acid to generate –COOH functional groups to their surface [6, 27]. It is well known that treatment of the CNTs with boiling nitric acid or other oxidants does not result in loss of the CNTs essential structural features (hydroxyl and carboxylic groups) [28]. In this work, we propose a two step process.

First step. SWCNTs (Applied Nanotechnologies, Inc. 90–95% purity) were dissolved in 15 mL of HNO_3 (Sigma-Aldrich, 70%). After 30 s of ultrasonication, the solution was refluxed at 120 °C under constant agitation for 8 h. The solid phase was removed by centrifugation. After being washed with deionized water, the recovered SWCNTs were dried at 70 °C for 24 h.

Second step. The obtained SWCNTs in the previous step were dissolved in 15 mL of HNO_3 (Sigma-Aldrich, 70%):deionized water (10:1). After 30 s of ultrasonication the solution was refluxed at 120 °C under constant agitation for 10 h. The solid phase was removed by centrifugation, after being washed with deionized water. Then, the treated SWCNTs were used for nanoparticles deposition *in situ* under inert atmosphere.

Synthesis of platinum nanoparticles

Platinum nanoparticles were obtained from $Pt_2(dba)_3$ precursor. This precursor was prepared according to the procedure reported by Moseley and Maitlis [29], using K_2PtCl_4 (Alfaesar, 99%) as raw material. Pt nanoparticles were synthesized and supported on SWCNTs *in situ* under inert atmosphere using schlenk techniques as follows: the $Pt_2(dba)_3$ precursor was added to distilled THF [26]. Thereafter, hexadecylamine, HDA (Fluka, 98%) (1 equivalent per Pt atom), and SWCNTs (70 equivalents per Pt atom) were added to the solution. Then, a dark brown suspension was obtained and pressurized under hydrogen atmosphere (3 bars) for 20 h and the suspension color turned from dark brown to a black suspension. The

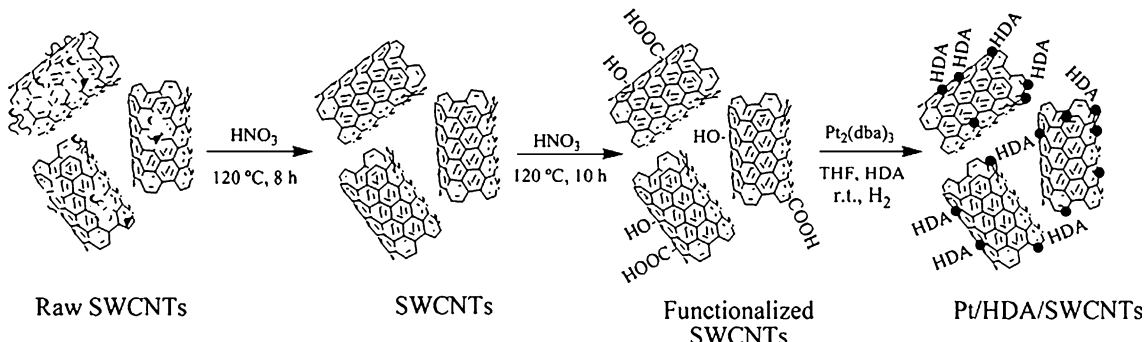


Fig. 1 Schematic process of the pretreatment of SWCNTs by nitric acid and subsequent decoration with Pt nanoparticles stabilized by hexadecylamine

resultant black suspension was purified by hexane washings until the solution turned colorless to eliminate the dibenzylideneacetone (yellow color) liberated from the decomposition of Pt₂(dba)₃ precursor and, finally, the purified black residue was dried under vacuum, Fig. 1.

Characterization of the Pt nanoparticles

Fourier transform-infrared spectroscopy (FT-IR, Spectrum One Perkin Elmer) was used to determine the presence and coordination of HDA on the surface of the Pt nanoparticles after purification steps, and also to confirm the presence of functional groups at the surface of pretreated SWCNTs, KBr pellets (Aldrich, 99% IR grade) were employed to carry out this analysis. Powder X-ray diffraction data of the sample was collected using a Brucker Advance D8 diffractometer with Cu K_α radiation, 0.02° min⁻¹ scan rate, from 2θ = 20° to 100°.

Morphological, dispersion, and average size studies were carried out by high resolution transmission electron microscopy (HRTEM, JEOL JEM-2010F Field Emission). A drop of the crude colloidal solution was deposited under argon on a holey carbon covered copper grid for TEM analysis.

Results and discussion

Figure 2a–d shows the FT-IR spectra of commercial SWCNTs, pre-treated (functionalized) SWCNTs, pure HDA, and Pt nanoparticles/HDA/pre-treated SWCNTs system, respectively. The spectra corresponding to commercial SWCNTs (Fig. 2a) and HDA (Fig. 2c) are presented as references.

As is shown in Fig. 2a, raw SWCNTs show no characteristic IR absorptions as reported previously [30, 31]. On the other hand, the band at 1585 cm⁻¹ (Fig. 2b) is assigned to the active carbon stretching mode of the SWCNTs-COOH [32]. There are also peaks around 1100 and

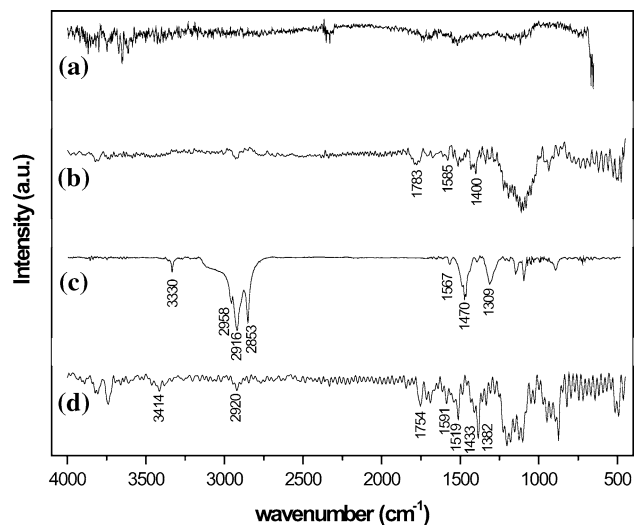


Fig. 2 FT-IR spectra of raw SWCNTs (a), functionalized SWCNTs (b), commercial HDA (c) and the system Pt nanoparticles/HDA/functionalized SWCNTs (d)

1160 cm⁻¹ corresponding to symmetric and asymmetric stretching bands of C—O—C of carboxylic groups according to Guzman et al. [23]. The band around 1400 cm⁻¹ is assigned to C—O stretching vibrations. Additionally, an absorption band at 1783 cm⁻¹ in the IR spectra indicates the formation of carboxylic groups on SWCNTs after the pretreatment [32]. Figure 3c exhibits the spectrum of pure HDA; from the FT-IR spectrum, the band $\nu_{\text{asymmetric}}$ ($-\text{CH}_2-$) at 2916 cm⁻¹, $\delta_{\text{asymmetric}}$ ($-\text{CH}_3$) at 1470 cm⁻¹ and $\delta_{\text{symmetric}}$ ($-\text{CH}_3$) at 1309 cm⁻¹; in Fig. 3d, the spectrum has some differences; these bands are shifted to 2920, 1519, and 1382 cm⁻¹, respectively. Additionally, the band ν_{NH} ($-\text{NH}_2$) at 3330 cm⁻¹ (Fig. 3c) corresponding to NH₂ stretching region shifted to 3414 cm⁻¹ (Fig. 3d) suggesting the coordination of $-\text{NH}_2$ group at the surface of Pt nanoparticles. This latter difference indicates a change occurs in the coordination environment between HDA pure and Pt nanoparticles/HDA/pre-treated SWCNTs system. This suggests that many of the alkylamines desorbed from

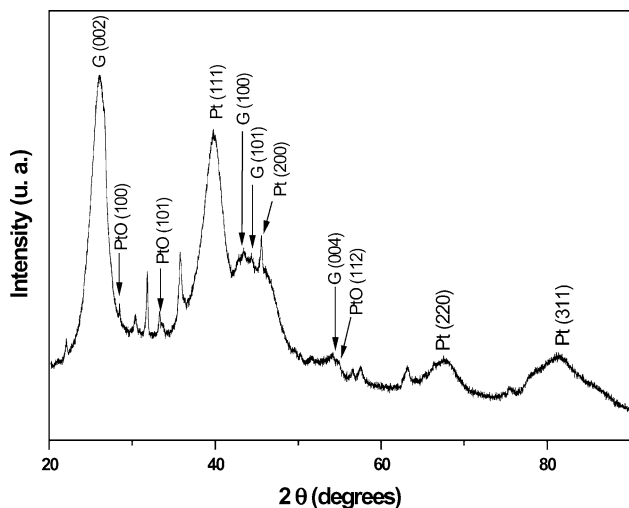


Fig. 3 Powder X-ray diffraction patterns of Pt nanoparticles/HDA/pre-treated SWCNTs system

the surface of SWCNTs because of the presence of carboxylic groups on SWCNTs [33]. Furthermore, the bands assigned to the active carbon stretching mode of the SWCNTs–COOH, C–O stretching vibrations and the band corresponding to the formation of carboxylic groups on SWCNTs (Fig. 3b) were also shifted to 1591, 1416, and 1754 cm^{-1} , respectively (Fig. 3d). It can be deduced from these results that the interaction between SWCNTs and HDA seems to be physical absorption and also no formation of ester bonds that could let a strong linkage with carboxylic groups of SWCNTs–COOH was observed [32].

The X-ray diffractogram of stabilized Pt nanoparticles/HDA/pre-treated SWCNTs system is shown in Fig. 3. The diffractogram contains very broad peaks at 39.7° , 45.5° , 67.6° , and 81.6° that can be assigned to Pt face-centered cubic (fcc) structure based on the data of the JCPDS file [04-0802] and corresponding to (111), (200), (220), and (311) crystalline planes, respectively. The SWCNTs

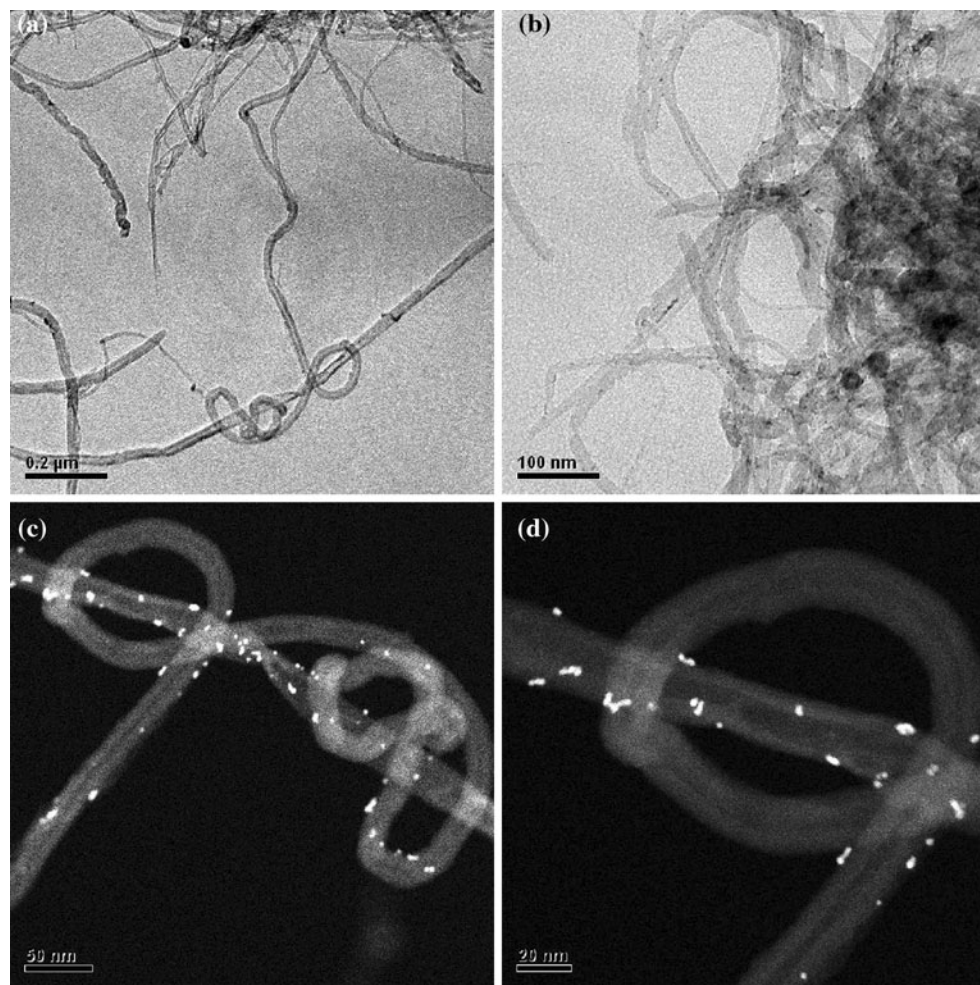


Fig. 4 TEM images of SWCNTs with dispersed Pt nanoparticles stabilized by HDA

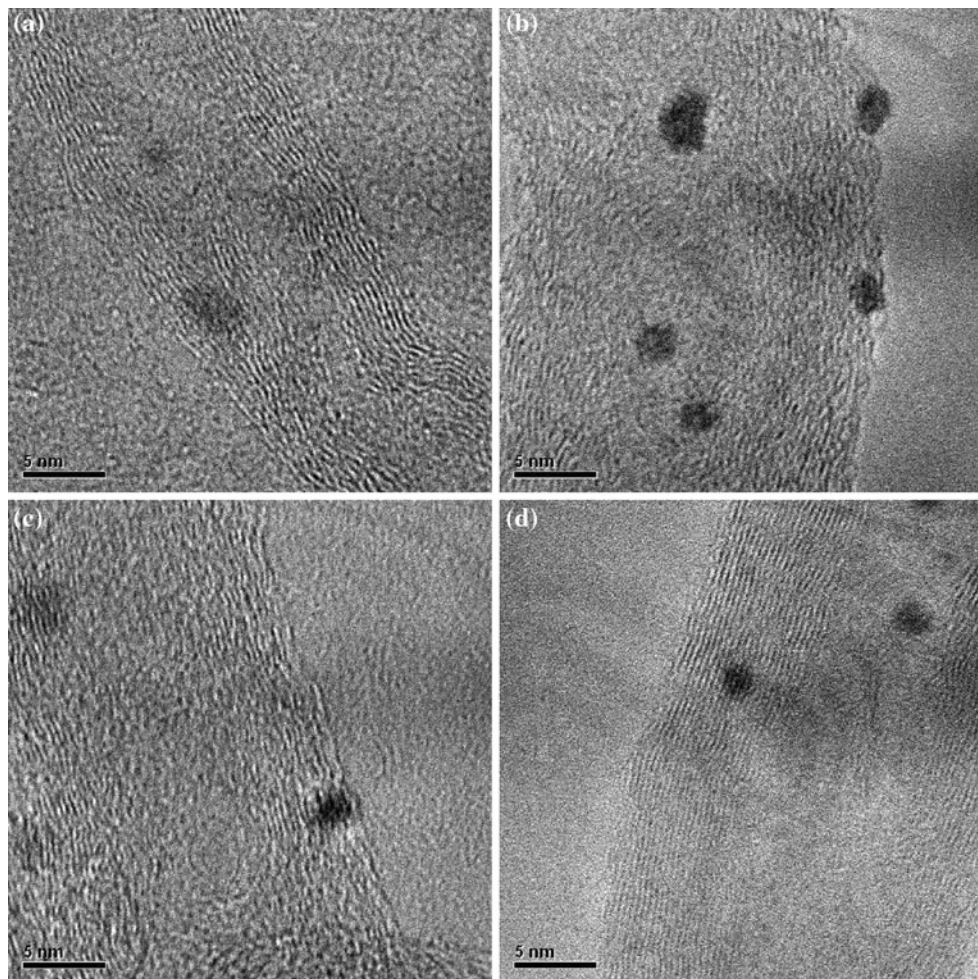


Fig. 5 HRTEM images of SWCNTs with dispersed Pt nanoparticles stabilized by HDA

showed the typical peak of the (002) phase of graphite [11, 34]. Additionally, some signals were assigned to PtO (JCPDS 43-1100) at 28.5°, 33.5°, and 54.8° corresponding to (100), (101), and (112) planes, this species could be produced on the surface during XRD analysis because the nanoparticles were exposed to the air. The rest of the signals were attributed to HDA employed as stabilizer, which was in a 1:1 ratio respect to Pt. Similar results (broad and overlapping peaks) between 35° and 50° (2θ) were reported by Bayrakceken with Pt/MWCNTs system synthesized from PtMe₂COD by supercritical carbon dioxide deposition analyzed without purification steps [10]. A full particle size analysis was not possible because the peaks are extremely broad, with the (111) and (200) from Pt and (100) and (101) from Graphite peaks overlapping, but an estimate of particle size was obtained from the (220) diffraction peak using Scherrer's equation (1):

$$t = \frac{0.9\lambda}{B \cos \theta_B} \quad (1)$$

where t is the mean particle size, λ is the X-ray wavelength (0.15405 nm for Cu K α), B is the full width-at-half-maximum (FWHM) height of a diffraction peak at Bragg angle θ .

The particle size obtained by Scherrer's equation was 2.5 nm. This result will be compared with that obtained by TEM analysis.

Figure 4a–d illustrates the representative transmission electron microscopy (TEM) in bright and dark field images of Pt nanoparticles/HDA/SWCNTs system. It can be seen from Fig. 4a–b that SWCNTs form bundles, as generally occur when they are suspended in solution [35]. Figure 4b shows a higher magnification view of a region where individual bundles of SWCNTs are visible. Additionally, two high magnification views in dark field micrographs are shown in Fig. 4c and d. Isolated Pt nanoparticles (Fig. 4c) and some coalesced particles forming nanowires of length 10–20 nm (Fig. 4d) are observed. Such coalescence of Pt nanoparticles into nanowires has been previously reported

in absence of SWCNTs studying the influence of HDA:metal ratio on the shape of Pt nanoparticles [26]. In this work, using 1 or 10 eq. of HDA, long polycrystalline nanowires with regular diameter (1.5–2 nm) were observed. NMR studies evidenced the coordination of the amine through the NH₂ group on the surface of the Pt nanoparticles. This coordination was associated to a fast exchange between free and coordinated amine molecules, leading to a temporary lack of amine onto the platinum nanoparticles surface, provoking a coalescence process of Pt nanoparticles producing long nanowires [26]. In the case of this work, under the same experimental conditions in the presence of 1 eq. of HDA, the presence of SWCNTs let to obtain isolated Pt nanoparticles and some nanowires of short length. SWCNTs stabilize the Pt nanoparticles avoiding the formation of long nanowires.

Additional HRTEM images are presented in Fig. 5a–d. It can be seen that Pt nanoparticles are well dispersed along SWCNT surfaces. The average platinum particle size was also determined from the HRTEM images to be about 2–3 nm, which is in agreement with the value calculated by Scherrer equation (2.5 nm). Despite the small size of the Pt particles, particle agglomeration is rare, thanks to the presence of HDA acting as a stabilizing agent, which contributes to the well dispersion of the Pt nanoparticles [26]. It seems that Pt nanoparticles tend to be preferentially attached where there is a larger concentration of carboxylic acid groups. The morphology of the particles was revealed more clearly in Fig. 5b and d exhibiting semispherical shape.

According to the HRTEM results, the preliminary mean particle size calculated using Scherrer's equation from XRD diffractograms (2.5 nm) presents a good agreement of that obtained from HRTEM micrographs (2–3 nm).

Conclusions

We have demonstrated that Pt nanoparticles can be obtained on functionalized SWCNTs by decomposition of the complex Pt₂(dba)₃ under H₂ in the presence of a long alkylchain amine (HDA). HRTEM studies revealed isolate Pt nanoparticles (2–3 nm) and nanowires (10–20 nm) were also observed on SWCNTs. The formation of nanowires seems to be influenced by coordinated amine molecules, indicating amine mobility and leading to a temporary lack of amine onto the platinum nanoparticles surface, giving rise to a lack of stability, and can provoke the nanoparticles coalescence process. However, the presence of SWCNTs limits the formation of longer nanowires in comparison with the synthesis carried out in the absence of SWCNTs observed in a previous work under the same conditions.

The synthetic method in this study may be highly promising as an alternative route to prepare small size Pt nanoparticles.

Acknowledgements The authors wish to acknowledge the financial support provided by CONACyT through 59921 and 2008-0838 SIP-Instituto Politécnico Nacional and 2009 projects. We also thank S. Tehuacanero of the Instituto de Física, Universidad Nacional Autónoma de México for the technical support in the TEM and HRTEM observations of the samples and F. Cervantes-Sodi of the Physics and Mathematics Department, Universidad Iberoamericana for their fruitful comments.

References

1. Saito R, Dresselhaus G, Dresselhaus MS (1998) Physical properties of carbon nanotubes. Imperial College Press, London
2. Reich S, Thomsen C, Maultzsch J (2004) Carbon nanotubes; basic concepts and physical properties. Wiley-VCH, Berlin
3. Dong L, Subramanian A, Nelson BJ (2007) Nanotoday 2:12
4. Sohn JI, Lee S, Kim H (2001) Appl Phys Lett 78:3130
5. Baughman RH, Zakhidov AA, de Heer WA (2001) Science 297:787
6. Zhao Y, Fan L, Zhong H, Li Y (2007) Microchim Acta 158:327
7. Prabhuram J, Zhao TS, Tang ZK, Chen R, Liang ZX (2006) J Phys Chem B 110:5245
8. Cao HQ, Zhu MF, Li YG (2006) J Solid State Chem 179:1208
9. He C, Zhao N, Shi C, Li J, Li H (2008) Mater Res Bull 43:2260
10. Bayrakceken A, Kitkamthorn U, Aindow M, Erkey C (2007) Scripta Mater 56:101
11. Guo D-J, Li H-L (2004) J Electroanal Chem 573:197
12. Zhao D, Han E, Wu X, Guan H (2006) Mater Lett 60:3544
13. Tang H, Chen JH, Huang ZP, Wang DZ, Ren ZF, Nie LH, Kuang YF, Yao SZ (2004) Carbon 42:191
14. Bonnemann H, Nagabushana KS (2004) J New Mater Electrochem Syst 7:93
15. Lee K, Zhang J, Wang H, Wilkinson DP (2006) J Appl Electrochem 36:507
16. Rajalakshmi N, Ryu H, Shajumon MM, Ramaprabhu S (2005) J Power Sources 140:250
17. Satishkumar BC, Vogl EM, Govindaraj A, Rao CNR (1996) J Phys D 29:3173
18. Guo D-J, Cui S-K (2008) J Solid State Electrochem 12:1393
19. Yen CH, Cui X, Pan HB, Wang S, Lin Y, Wai CM (2005) J Nanosci Nanotechnol 5:1852
20. Liang Y, Li J, Wang SZ, Fu XZ, Xu QC, Lin JD, Liao DW (2008) Catal Lett 120:236
21. Zhang L, Cheng B, Samulski ET (2004) Chem Phys Lett 398:505
22. Tzitzios V, Niarchos D, Gjoka M, Boukos N, Petridis D (2005) J Am Chem Soc 127:13756
23. Guzmán C, Orozco G, Verde Y, Jiménez S, Godínez LA, Juaristi E, Bustos E (2009) Electrochim Acta 54:1728
24. Solla Gullón J, Lafuente E, Aldaz A, Martínez MT, Feliu JM (2007) Electrochim Acta 52:5582
25. Chaudret B (2005) C R Physique 6:117
26. Ramirez E, Eradès L, Philippot K, Lecante P, Chaudret B (2007) J Adv Funct Mater 17:2219
27. Lordi V, Yao N, Wei J (2001) Chem Mater 13:733
28. Tsang SC, Harris PJF, Green MLH (1993) Nature 362:520
29. Moseley K, Maitlis PM (1971) J Chem Soc D 982–983
30. Guo Z, Liang L, Liang J-J, Ma Y-F, Yang X-Y, Ren D-M, Chen Y-S, Zheng J-Y (2008) J Nanopart Res 10:1077

31. Li H-M, Cheng F-Y, Duft AM, Adronov A (2005) J Am Chem Soc 127:14518
32. Shi Q, Yang D, Su Y, Li J, Jiang Z, Jiang Y, Yuan W (2007) J Nanopart Res 9:1205
33. Ibañez FJ, Zamborini FP (2008) J Am Chem Soc 130:622
34. Terrones M, Hsu WK, Schilder A, Terrones H, Grobert N, Hare JP (1998) Appl Phys A 66:307
35. Wang JI, Yin GP, Zhang J, Wang ZB, Gao YZ (2007) Electrochim Acta 52:7042